Heliyon 10 (2024) e38488

Contents lists available at ScienceDirect

Heliyon

journal homepage: www.cell.com/heliyon

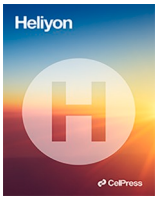

Research article

Identification of molecular subtypes, prognostic status and immunotherapy response in cervical cancer based on angiogenic signature genes

Zhuo Deng, Lu Zhang, Chenyang Sun, Yiping Liu, Bin Li *

Department of Gynecology, Shaanxi Provincial People's Hospital, Xi'an, 710000, China

ARTICLE INFO

Keywords:
Cervical cancer
Angiogenesis
Molecular subtyping
Prognosis
Immunotherapy

ABSTRACT

Background: Cervical cancer, as one of the most common malignancies in women, is closely related to the mechanism of angiogenesis, which needs further exploration.
Methods: The squamous cell carcinoma of the cervix and cervical adenocarcinoma (CESC) data from The Cancer Genome Atlas (TCGA) database. CESC subtypes based on 48 angiogenesis-related genes were identified using consistent cluster analysis, and the limma package were adopted to screen the differentially expressed genes (DEGs) associated with prognosis. Further compress the DEGs through univariate and Least Absolute Shrinkage and Selection Operator (LASSO) COX analysis to identify the key genes. Calculate immune scores using the GSVA package and predict immunotherapy response with TIDE. For *in vitro* analysis, the expressions of these key genes were additionally tested via reverse-transcription quantitative PCR, and the migration and invasion of Hela cells were determined in scratch and transwell assays, respectively.
Results: 3 CESC subtypes were identified, with the best survival advantage in the C2 subtype and the worst in C1 subtype. A risk model was established utilizing seven key genes (MMP3, DLL4, CAP2, PDIA6, TCN2, PAPSS2, and VCAM1), showcases an Area Under the Curve (AUC) exceeding 0.7, underlining its robust performance. The risk score model showed a trend of poorer survival for patients in the high-risk score group and good agreement across different datasets. A nomogram was constructed, and calibration curves indicated robust predictive performance. Immunological analysis revealed heightened sensitivity to immunotherapy in the low-risk group. Besides, the elevated expressions of all 7 genes were seen in Hela cells, and the specific target-mediated DLL4 knockdown diminished the migration and invasion of Hela cells *in vitro*.
Conclusion: This research provides fresh insights and a valuable tool to guide therapeutic decision-making for CESC.

1. Introduction

Cervical cancer ranks the fourth in the most prevalent female cancer across the globe, with around 660,000 reported new cases in 2022. The disease is particularly common among women in nations with low and middle income, largely because of significant disparities in access to human papillomavirus (HPV) vaccination, screening, and treatment services in these regions [1,2]. HPV is a double-stranded circular DNA virus that is closely related to the development of cervical cancer [3]. Studies have found that HPV can

* Corresponding author.
E-mail address: syylibin@163.com (B. Li).

https://doi.org/10.1016/j.heliyon.2024.e38488
Received 26 July 2024; Received in revised form 24 September 2024; Accepted 25 September 2024
Available online 26 September 2024

infect the basal epithelial cells of the mucosal membrane [4], and HPV lesions are caused by unchecked cell proliferation and mutations, ultimately leading to cancer [5]. In the United States, 13,960 new cases and approximately 4310 deaths from the disease are expected in 2023, with higher rates among Hispanic/Latino, black, and Asian populations [6,7]. Both cancer stage and individual factors can be the determinants for the treatment of cervical cancer, and the main treatment modalities mainly consist of surgery and other regimens like radiation therapy, chemotherapy, targeted therapy, and immunotherapy. Surgical resection is usually used for small, localized cancers, which ranges from minor fertility preserving surgery to more extensive procedures such as radical hysterectomy, depending on the spread of the cancer and the patient's future reproductive plans. Radiation therapy is usually applied in conjunction with chemotherapy for cancers that extend beyond the cervix or to reduce the risk of recurrence after surgery [8–11]. Targeted therapies and immunotherapy, which target specific chemicals in cancer cells or strengthen the ability of the immune system to kill the malignant cells, are commonly used to treat advanced cervical cancer. Despite advances in treating and screening for cervical cancer, significant challenges remain in the fight against the disease. The diverse presentations of cervical cancer and high individual variability in patient response to treatment require more personalized diagnostic and therapeutic approaches [12–14]. Effective screening programs are critical but underutilized, especially in resource-poor settings. Despite the reduction in the incidence rate following the introduction of HPV vaccines, the incomplete coverage remains an urgency in developing countries [15].

The role of angiogenesis in cancer is primarily to support tumor growth, progression, and metastasis through the formation of new vascular networks. This process involves neovascularization from existing blood vessels and is one of the key factors in tumor development [16–18]. In cancer therapy, anti-angiogenic drugs are used to inhibit the blood supply to tumors by blocking factors that promote angiogenesis, thereby limiting tumor growth and spread. These drugs mainly target vascular endothelial growth factor (VEGF) and its receptors, as VEGF is one of the most important pro-angiogenic factors. Although antiangiogenic treatments have been widely used in the clinic, their effects only temporarily prolong the survival of patients sometimes, and the adaptation and resistance of tumors to such treatments are the focus of current research [19]. For example, tumors may bypass inhibition of the VEGF pathway by upregulating other pro-angiogenic pathways. In addition, some studies are exploring strategies to combine anti-angiogenic drugs with chemotherapy or immunotherapy to improve treatment efficacy [20,21]. Anti-angiogenic agents such as bevacizumab have been approved for use in cervical cancer research, but due to their toxicity rate, further research is needed [22]. Considering the essential role angiogenesis in cancer, anti-angiogenic therapies targeting this process, although promising, still face many challenges, including the durability of the therapeutic effect and the problem of tumor adaptation. Solutions to these challenges require more in-depth research and the development of new therapeutic strategies.

Here, we comprehensively analyzed angiogenesis-related genes in cervical cancer, identified the molecular subtypes in which angiogenesis is characterized and constructed a prognostic assessment model. We hope these relevant results not only provide new insights into the molecular classification of cervical cancer, but also lays a theoretic foundation for clinical prognostic assessment and the development of personalized therapeutic strategies through risk scoring models.

2. Methods

2.1. Data sources and pre-processing

Relevant data on cervical squamous cell carcinoma and endocervical adenocarcinoma (CESC) were downloaded from The Cancer Genome Atlas (TCGA, https://portal.gdc.cancer.gov/) database for sequencing analysis (TCGA-CESC). This dataset contains FPKM

Table 1
Statistical analysis of clinical information for samples in the training and validation sets.

Characteristics	Train(N = 204)	Test(N = 87)	Total(N = 291)	pvalue	FDR
Age					
Mean ± SD	47.76 ± 13.53	48.86 ± 14.48	48.09 ± 13.81		
Median[min-max]	46.00[20.00,85.00]	47.00[25.00,88.00]	46.00[20.00,88.00]		
Gender					
FEMALE	204(70.10 %)	87(29.90 %)	291(100.00 %)		
AJCC_stage				0.24	0.48
I	115(40.35 %)	44(15.44 %)	159(55.79 %)		
II	47(16.49 %)	17(5.96 %)	64(22.46 %)		
III	27(9.47 %)	14(4.91 %)	41(14.39 %)		
IV	11(3.86 %)	10(3.51 %)	21(7.37 %)		
Grade				0.54	0.54
G1	14(5.30 %)	4(1.52 %)	18(6.82 %)		
G2	94(35.61 %)	35(13.26 %)	129(48.86 %)		
G3	77(29.17 %)	39(14.77 %)	116(43.94 %)		
G4	1(0.38 %)	0(0.0e+0 %)	1(0.38 %)		
OS					
Mean ± SD	0.25 ± 0.44	0.22 ± 0.42	0.24 ± 0.43		
Median[min-max]	0.0e+0[0.0e+0,1.00]	0.0e+0[0.0e+0,1.00]	0.0e+0[0.0e+0,1.00]		
OS.time					
Mean ± SD	1116.67 ± 1199.34	987.46 ± 1025.20	1078.04 ± 1149.82		
Median[min-max]	747.00[3.00,6408.00]	642.00[2.00,4483.00]	715.00[2.00,6408.00]		

expression profiling information of RNA-Seq samples. The RNA-Seq data from TCGA-CESC were processed as follows [1]: Only samples with survival time and survival status were retained, while those lacking such information were removed [2]. Ensembl was converted to Gene symbol [3]. The expression matrix was transferred to the TPM format and log2 transformation was carried out [4]. The protein-coding genes were reserved. Finally, 291 CESC samples were obtained. The 48 angiogenesis-related genes were also collected utilizing the Molecular Signatures Database (MSigDB, https://www.gsea-msigdb.org/gsea/msigdb) database.

2.2. Consensus clustering analysis

In the TCGA-CESC cohort, in accordance with the expression profiles of 48 angiogenesis-related genes, 291 CESC samples were analyzed for angiogenesis-related molecular subtypes by consistency clustering analysis with the ConsensusClusterPlus package [23]. For the analysis, the parameters were set to clusterAlg = "km", distance = "euclidean", and the sampling was repeated 500 times with a sampling proportion of 80 % each time. For the molecular subtypes obtained from the cluster analysis, in order to identify differentially expressed genes (DEGs) in each subtype, the DEGs among them were recognized by the limma package, which were considered only when satisfying FDR <0.05 & $|\log2FC| > 1.5$ [24].

2.3. RiskScore construction and validation

First, the training and validation sets of TCGA-CESC cohort were divided in the ratio of 7:3 by random grouping. Based on the clinical information, the reasonableness of the randomized grouping was verified using chi-square test. The detailed statistical information in these two sets is displayed in Table 1. Univariate COX analysis was performed on the DEGs of the training set then to extract those significantly associated with the prognosis of cervical cancer ($p < 0.05$). Then glmnet package was applied to perform Least Absolute Shrinkage and Selection Operator COX (LASSO COX) analysis [25] to ascertain the independent prognostic factors. The key prognostic genes were finally obtained, and the RiskScore of the samples was calculated using the risk coefficient and gene expression level via the following formula:

$$\text{RiskScore} = \Sigma\beta i \times \text{Expi}$$

β is the risk coefficient of the prognostic gene, and Exp is the expression data of the prognostic gene.

The samples were allocated into high and low RiskScore groups based on the median value of RiskScore, followed by the Kaplan-Meier survival analysis. Besides, the constructed Receiver Operating Characteristic curve (ROC) was plotted by timeROC package [26] to assess the accuracy of RiskScore in predicting the prognosis of Cervical cancer patients by Area Under the Curve (AUC).

2.4. Immune microenvironment assessment

A set of 27 immune cell-related genes from the study by He et al. [27] was extracted, and samples in TCGA-CESC were enriched for gene set analysis to assess immune cell activity and infiltration abundance in the tumor microenvironment (TME) of the samples by the GSVA package [28]. We also assessed StromalScore, ImmuneScore, and ESTIMATEScore in all samples by the ESTIMATE algorithm [29].

2.5. Immunotherapy sensitivity analysis

The Tumor Immune Dysfunction and Exclusion (TIDE) score is a biomarker predicting the response of cancer patients to immune checkpoint inhibitory therapies like PD-1/PD-L1 and CTLA-4 inhibitors. This scoring system is based on the immune status in the tumor microenvironment, taking into account, in particular, immune cell function and mechanisms of escape of tumor cells from the immune system. A high TIDE score indicates that a patient's tumor may be less sensitive to immune checkpoint inhibitors because of more immune dysfunction or immune exclusion in their TME, whereas a low TIDE score predicts that the patient may respond better to treatment [27]. The Immunopheno score (IPS) is a biomarker for assessing a tumor's response to immune checkpoint blocking therapies (PD-1/PD-L1 and CTLA-4 inhibitors) as a tool for assessing a tumor's likely response. This scoring system focuses on analyzing the immune phenotype in the TME and incorporates expression data of effector T-cell markers, antigen presentation mechanisms, and immunosuppressive factors to predict treatment efficacy. Higher IPS scores generally imply that the tumor has stronger immune visibility and a less immunosuppressive environment, thus more likely responding positively to immune checkpoint inhibitor therapy [30]. We assessed the TIDE score of all samples by the TIDE algorithm and calculated the IPS score of all samples by the IOBR package [31].

2.6. Cell culture and transfection

Human cervical epithelial cell (HcerEpic, CP-H059) and cervical cancer cell line Hela (CL-0101) were all purchased from Pricella (Wuhan, China). The culture media for these two cells were minimal essential medium (11430030, Gibco, Grand Island, NY), which were additionally added with 10 % fetal bovine serum (A3161001C, Gibco) and 1 % penicillin-streptomycin (15070063, Gibco) at 37 °C, 5 % CO_2. For the subsequent transfection via liposome, Hela cells were grown in a 6-well plate at 1×10^6 cells per well and received the transfection of commercial small interfering RNA against DLL4 (target sequence: 5′-GCCAACTATGCTTGTGAATGTCC-3′)

or the negative control small interfering RNA at 37 °C for 48 h. All cells were collected then for the subsequent scratch and transwell assays.

2.7. Reverse-transcription quantitative PCR on mRNA levels

The total RNA extractor TriZol (15596026, Invitrogen, Carlsbad, CA) was adopted to extract the total cellular RNA from both HcerEpic and Hela cells, following which the concentration of extracted RNA was tested in the spectrophotometer. A corresponding cDNA synthesis kit (B300902, Sangon Biotech, Shanghai, China) was adopted for the synthesis of corresponding cDNA. Thereafter, the SYBR Green PCR Mix (B110031, Sangon Biotech) and the CFX396 touch PCR system were used for the PCR analysis at the following parameters: 95 °C for 3 min and 40 cycles of 94 °C for 15 s, 60 °C for 30 s and 72 °C for 1 min. The relative mRNA expression level was finally calculated using the method $2^{-\Delta\Delta CT}$ with GAPDH as the housekeeping control [32,33]. The sequences of primers in this study were shown in Table 2.

2.8. Scratch assay

CC cells Hela (1×10^6 cells/mL) were seeded in 6-well plates and grown until fully confluent. Subsequently, a 10 μL sterile pipette tip was applied to create a scratch on the monolayer and cells were continued for the 48-h culture. Following the rinse in PBS to remove the debris, cells were observed in the IX71 inverted microscope (Olympus, Tokyo, Japan) and the wound closure degree was hereafter determined.

2.9. Transwell assay

CC cells Hela (2×10^5 cells in total) were placed in the upper Transwell chamber (pore: 8.0 μm, 3422, Corning, Inc., Corning, NY) coated with Matrigel matrix (M8370, Solarbio, Beijing, China) and added with 200 μL serum-deprived media. The lower chamber was filled with 600 μL serum-added media in the meantime. 48 h later, the invaded cells were fixed and dyed using 4 % paraformaldehyde (P1110, Solarbio) and 0.1 % crystal violet (E607309, Sangon Biotech). The inverted microscope (Olympus) was adopted to calculate the number of invaded cells.

2.10. Statistical analysis

All computational analyses were realized through R software (version 3.6.0), and GraphPad Prism software (version 8.0.2) was applied for the statistical analyses. The student's t-test was adopted to compare the mRNA expression levels of key genes between tumor samples and control samples in the *in vitro* validation experiment. The data with $p < 0.05$ were statistically significant in all statistical analyses.

3. Results

3.1. Cervical cancer subtypes based on angiogenesis-related genes

First, in the TCGA-CESC dataset, a consistent clustering analysis was performed based on the expression data of 48 angiogenesis-related genes. CESC can be intuitively identified into three subtypes. The best and worst survival advantage were seen in the C2 subtype and C1 subtype, respectively (Fig. 1A). Based on Univariate COX analysis, 10 of 48 angiogenesis-related genes were associated with the prognosis of CESC, including SERPINF1, ANGPTL4, RHOB, CXCL8, COL4A2, PF4, VEGFA, C1GALT1, CANX, and PROK2 (Fig. 1B). Moreover, C1 subtypes in the majority of patients were in intermediate and advanced stages (Stage III, Stage IV, and G3), and

Table 2
Primers for reverse-transcription PCR.

Gene	NCBI Accession Number	Primers (5′-3′)	
		Forward	Reverse
MMP3	NM_002422.5	CACTCACAGACCTGACTCGGTT	AAGCAGGATCACAGTTGGCTGG
VCAM1	NM_001078.4	TCTACGCTGACAATGAATC	CTTATGTCCACAAGTCACTG
DLL4	NM_019074.4	CTGCGAGAAGAAAGTGGACAGG	ACAGTCGCTGACGTGGAGTTCA
CAP2	NM_006366.3	GCCTCTCAGTACCAACAA	TACTCCACTCTCCATTTCTT
TCN2	NM_000355.4	CAGAACAGTGCGAGAGGAGATC	TCGCCTTGAGACATGCTGTTCC
PDIA6	XM_011510308.2	ACAAGGCAGAAGTGATAGTT	ATCACTGAGGTCAATGTCA
PAPSS2	NM_004670.4	AGGAACGCTGTTCCCGTGTTTG	GAGGTGTCAGACGGTATTGGTC
BCL-2	NM_000633.3	CCGCATCAGGAAGGCTAGAGTT	CCAGACATTCGGAGACCACACT
CDK6	NM_001259.8	TGGTGACCAGCAGCGGACAA	GCAGCCAACACTCCAGAGATCC
PDCD4	NM_014456.5	GCGATTCGGTCAGCGACAGT	CACATCCACCTCCTCCACATCA
PTEN	NM_000314.8	TTGAGAGTTGAGCCGCTGTGAG	TCAGGAGAAGCCGAGGAAGAGG
GAPDH	NM_002046.7	GTCTCCTCTGACTTCAACAGCG	ACCACCCTGTTGCTGTAGCCAA

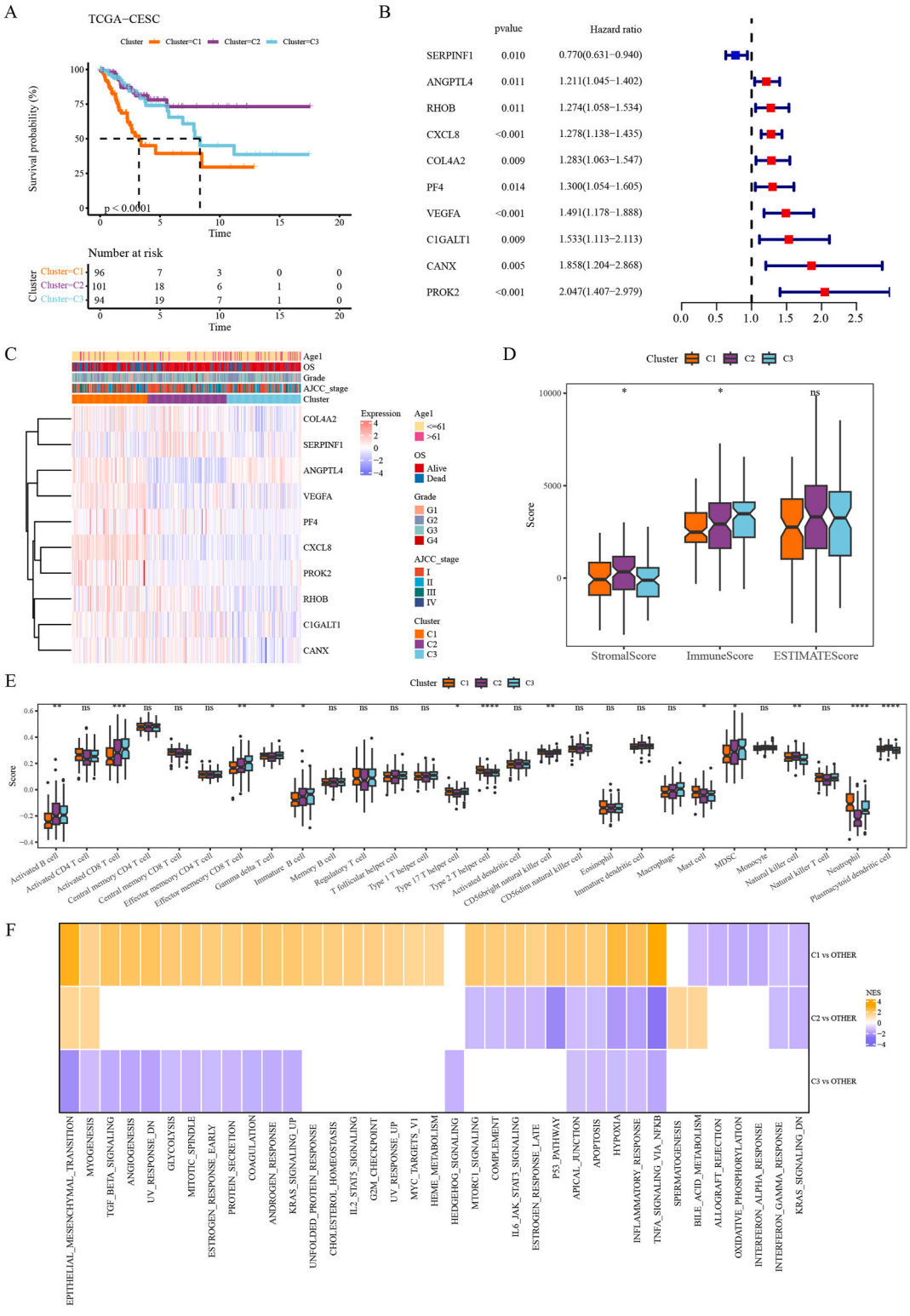

Fig. 1. Prognostic, expression, immune, and biological pathway characterization in the three angiogenic signature subtypes.
A: Kaplan-Meier curves of patients in the C1, C2, and C3 subtypes. B: Multivariate COX analysis to identify prognostic genes for angiogenic features in CESC. C: Heatmap showing clinical information of patients in the three subtypes and expression levels of 10 prognostic genes characterized by angiogenesis. D: ESTIMATE results for the three subtypes. E: 27 immune cell activity scores in the three subtypes. F: Heatmap demonstrating biological pathways that are abnormally activated or inhibited in the C1, C2, and C3 subtypes.

the increased levels of 10 angiogenesis-related genes were also seen in the C1 subtype (Fig. 1C). ESTIAMTE immune infiltration analysis demonstrated the relatively higher ImmuneScore and ESTIMATEScore of C1 subtype (Fig. 1D). For the C2 subtype, cell activity of activated B cell was higher (Fig. 1E). In comparison with the other two subtypes, multiple cancer-relevant pathways were activated in the C1 subtype, like TGF_BETA_SIGNALING, ANGIOGENESIS, G2M_CHECKPOINT, IL6_JAK_STAT3_SIGNALING, KRAS_SIGNALING_UP (Fig. 1F).

3.2. Prognostic assessment models for angiogenic characterization in CESC

The relevant DEGs in the C1 (C1 vs C2&C3), C2 (C2 vs C1&C3), and C3 (C3 vs C1&C2) subtypes were sorted out (FDR <0.05&$|\log2FC| > 1.5$), respectively. In the C1 subtype, 595 DEGs were found, with 472 up-regulated and 123 down-regulated DEGs. 1374 DEGs were identified in the C2 subtype, including 950 up-regulated and 424 down-regulated DEGs. 1191 DEGs were discovered in the C3 subtype, which consisted of 211 up-regulated and 980 down-regulated DEGs. A total of 68 overlapping DEGs were intersected in the three subtypes (Fig. 2A). In the training set, 16 genes associated with CESC prognosis were initially identified following the univariate COX analysis in conjunction with patients' survival information ($p < 0.05$). After LASSO COX analysis, the overfitting genes were removed by penalizing the parameters and model training. The optimal λ value occurs when the number of features is 15, with a λ value of 0.03296859, which translates to −3.4122 after log transformation (Fig. 2B and C). 7 key genes affecting CESC prognosis, that is, TCN2, VCAM1, MMP3, CAP2, DLL4, PDIA6, and PAPSS2, were obtained (Fig. 2D). Based on the expression levels and risk coefficients of the seven prognosis-related genes, we constructed a risk model for predicting CESC prognosis.

$$\text{RiskScore} = 0.108*\text{MMP3} + 0.542*\text{DLL4} + 0.408*\text{CAP2} + 0.43*\text{PDIA6} - 0.813*\text{TCN2} + 0.281*\text{PAPSS2} - 0.237*\text{VCAM1}$$

Thereafter, the samples in the training set are grouped according to their median RiskScore values (high and low RiskScore group). Visibly, the relatively higher expression levels of MMP3, CAP2, DLL4, PDIA6, PAPSS2 were noted in the high RiskScore group, whilst the relatively higher expressions of TCN2 and VCAM1 were observed in the low RiskScore group (Fig. 2D).

Subsequently, the guidance of RiskScore on CESC prognosis was validated in the two sets, respectively. In the training set, the Kaplan-Meier curves of patients in both groups depicted the better survival in patients with low RiskScore (Fig. 3A). According to the

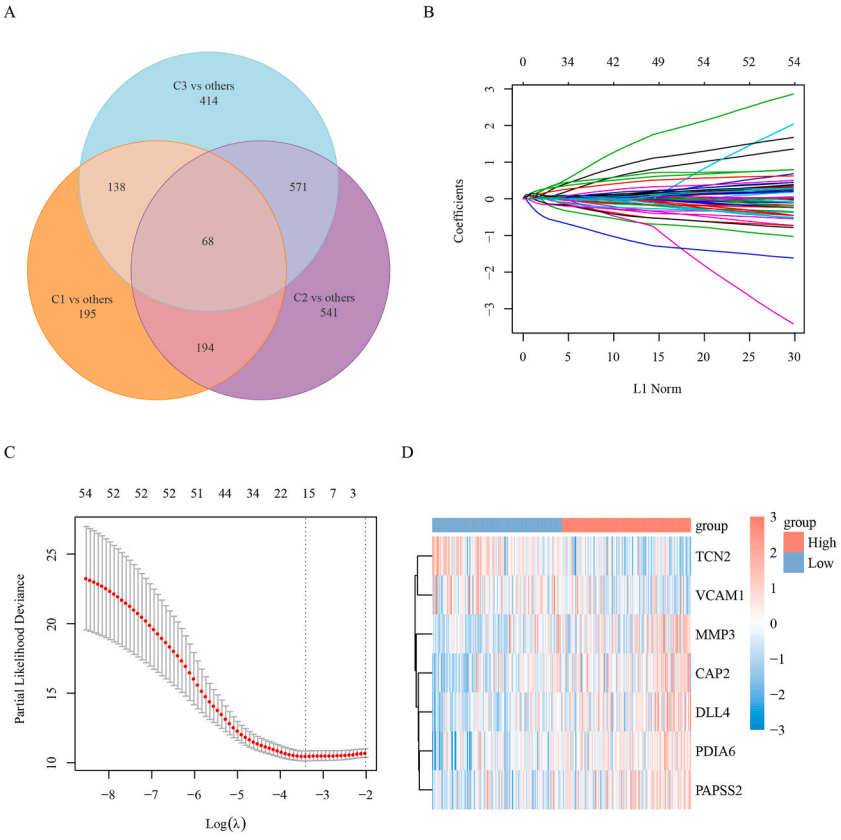

Fig. 2. Identification of prognostically relevant genes in CESC.
A: The Venn diagram showing the DEGs and overlapping DEGs in C1 (C1 vs C2&C3), C2 (C2 vs C1&C3), and C3 (C3 vs C1&C2). B: Trajectory plot of the coefficient change of the independent variables (genes) in the LASSO COX analysis. C: Confidence intervals for penalty parameter selection in LASSO COX analysis. D: Heatmap of expression levels of seven prognosis-related genes in high and low RiskScore groups.

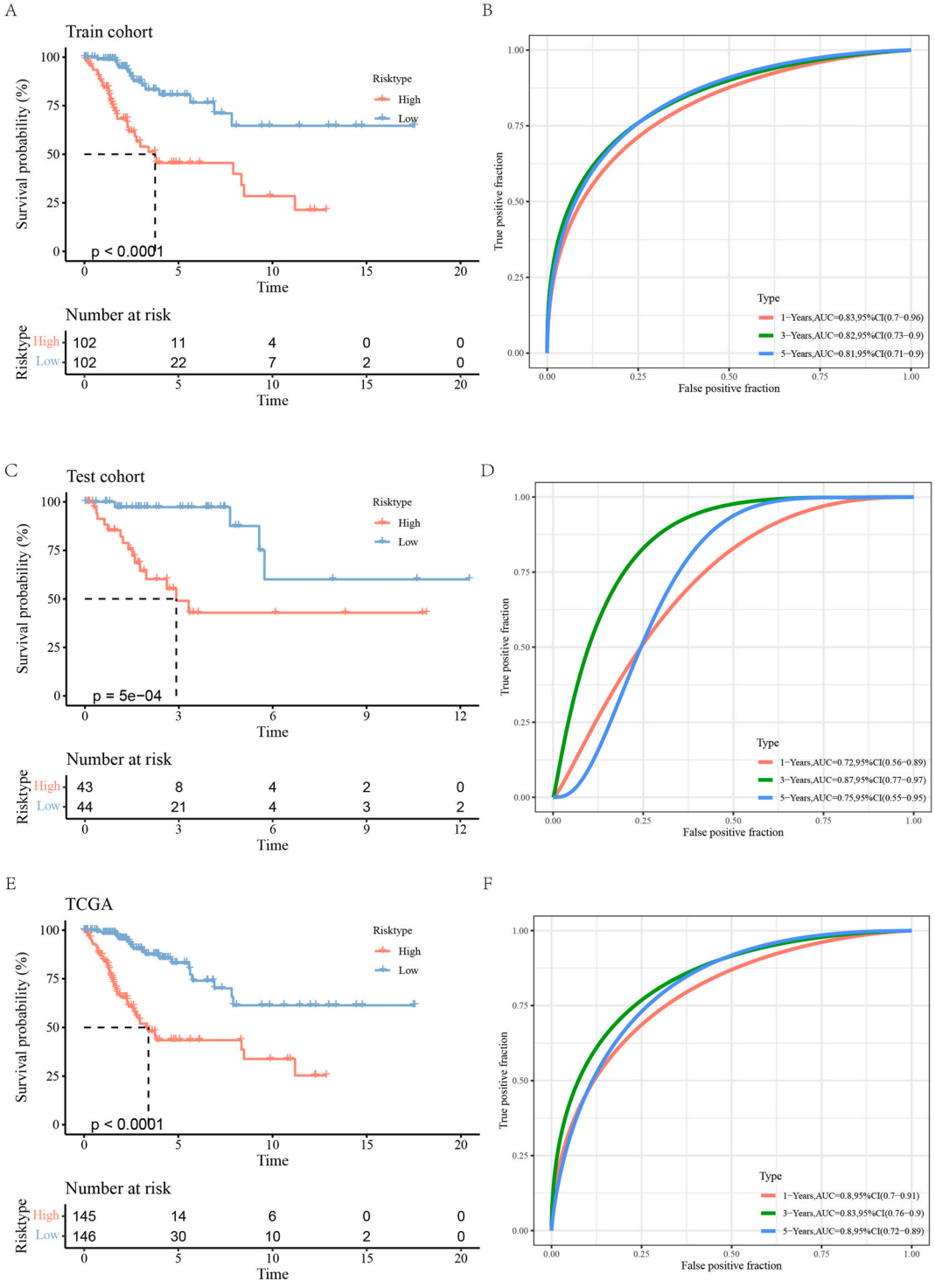

Fig. 3. Prognostic value assessment of RiskScore.
A: Kaplan-Meier curves of patients in high and low RiskScore groups in the training set. B: ROC curve showing the efficacy of the RiskScore in predicting the 1-, 3- and 5-year survival of CESC patients in the training set. C: Kaplan-Meier curves of patients in the high and low RiskScore groups in the validation set. D: ROC curve showing the efficacy of the RiskScore in predicting the 1-, 3- and 5-year survival of CESC patients in the validation set. E: Kaplan-Meier curves of patients with high and low RiskScore groupings in the entire TCGA-CESC cohort. F: ROC curve showing the efficacy of the RiskScore in predicting the 1-, 3- and 5-year survival of CESC patients in the entire TCGA-CESC cohort.

ROC curve, the AUC values of RiskScore for predicting 1-, 3-, and 5-year survival in CESC patients were 0.83, 0.82, and 0.81, respectively (Fig. 3B). In the validation set, a similar trend on the survival was seen in patients with low RiskScore (Fig. 3C). Higher AUC values for 1-, 3-, and 5-year survival prediction were also seen, including 0.72, 0.87, and 0.75 (Fig. 3D). Finally, the performance of RiskScore on prognostic assessment was validated in entire TCGA-CESC cohort, and the results were consistent with the trends in the two sets (Fig. 3E). The AUC values of RiskScore for predicting 1-, 3-, and 5-year survival of CESC patients in the TCGA-CESC cohort were 0.8, 0.83, and 0.8 (Fig. 3F). These results indicate that RiskScore is clearly a reliable prognostic assessment tool.

3.3. Potential clinical applications of RiskScore

In the TCGA-CESC cohort, the Age, AJCC stage, Grade, and RiskScore information of all samples were integrated. Both univariate COX and multivariate COX analyses were commenced to identify independent prognostic factors for CESC. A nomogram was accordingly plotted. Based on the univariate COX analysis results, the AJCC stage ($p < 0.01$, HR = 2.31,95 % CI = 1.43–3.78) and RiskScore ($p < 0.001$, HR = 2.45, 95 % CI = 1.96–3.07) could be used as independent prognostic factors for CESC (Fig. 4A). The multivariate COX analysis results also confirmed that AJCC stage and RiskScore were independent prognostic factors for CESC (Fig. 4B). Therefore, we constructed a nomogram for predicting 1-, 3-, and 5-year survival rates in CESC patients using RiskScore and AJCC stage (Fig. 4C). In TCGA-CESC cohort, calibration curves were plotted by combining the actual survival rates of patients and the predicted survival rates of the nomogram. The results manifested that the deviation between the actual observed and the predicted values was small and that the curves nearly overlapped (Fig. 4D). These results hinted the good potential of the nomogram for clinical prediction.

3.4. RiskScore for predicting immunotherapy response in CESC patients

The differences in immune microenvironment activity of patients in the high and low RiskScore groups were further compared.

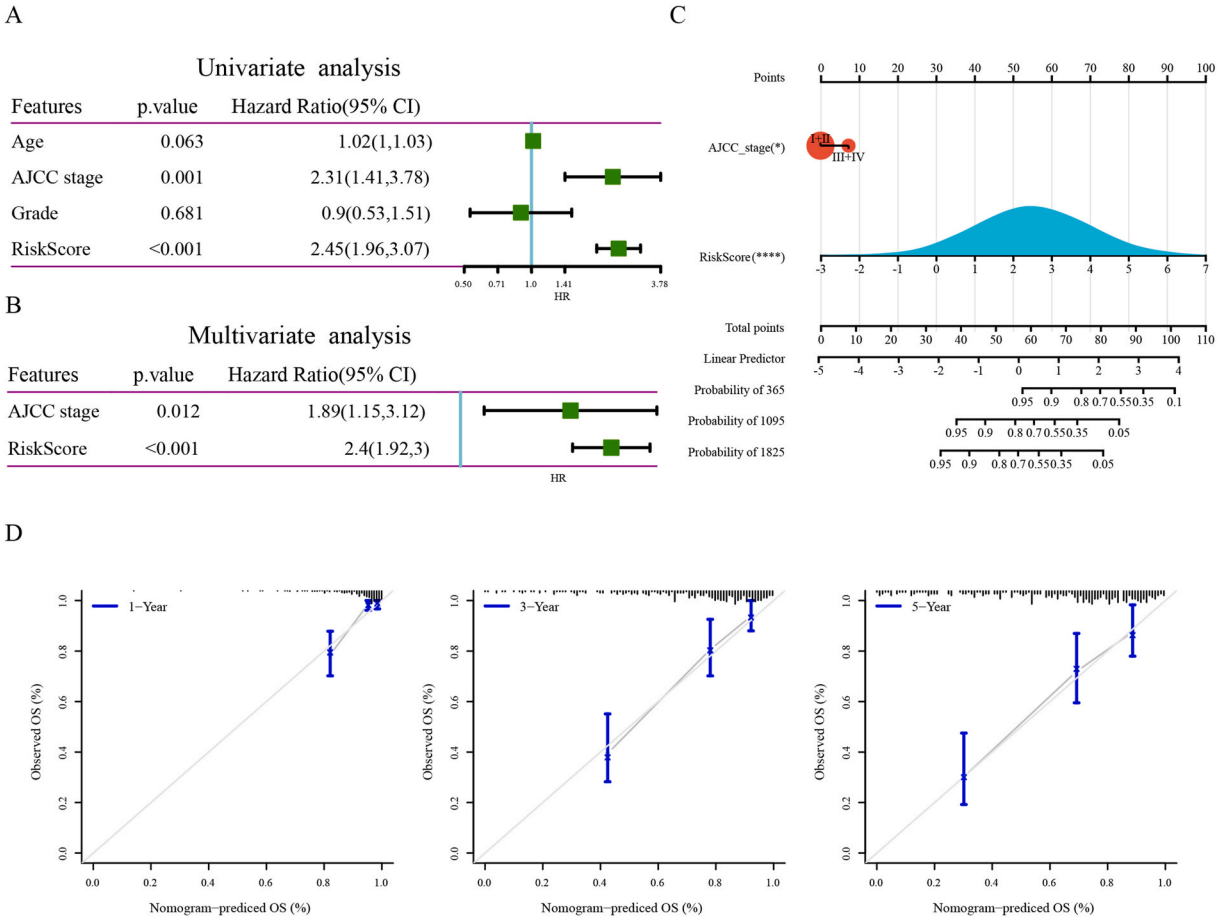

Fig. 4. Prognostic independence and nomogram for AJCC stage and RiskScore.
A-B: Univariate and multivariate COX analysis of RiskScore combined with clinical information. C: Nomogram containing the RiskScore and AJCC stage characteristics. D: Calibration curve to assess the prognostic performance of the nomogram.

Patients in the low RiskScore group exhibited a higher ImmuneScore and ESTIMATEScore (Fig. 5A). The level of immune cell infiltration of samples was also evaluated, and a higher level of immune cell infiltration in the TME of samples was observed in comparison with that in the low RiskScore group (Fig. 5B). Patients in the low RiskScore group exhibited low levels of TIDE scores, suggesting that this type of patient is more sensitive to immunotherapy (Fig. 5C). This was confirmed by the proportion of patients in the high and low RiskScore groups who responded to immunotherapy, and the response of patients in both groups after receiving immunotherapy was counted. The proportion of patients who benefited from immunotherapy was higher in the low RiskScore group (40 % in low RiskScore) (Fig. 5D). In addition, the higher proportion of patients with high IPS scores in the low RiskScore group was visualized. Higher IPS scores reflect a more favorable tumor immune microenvironment in which T cells may have been activated and able to effectively recognize and attack tumor cells, suggesting that patients in the low RiskScore group may be more sensitive to immunotherapy (Fig. 5E and F). Collectively, it was demonstrated that RiskScore may be useful for predicting the response of CESC patients to immunotherapy, and patients with low RiskScore in particular may be more likely to benefit from immunotherapy.

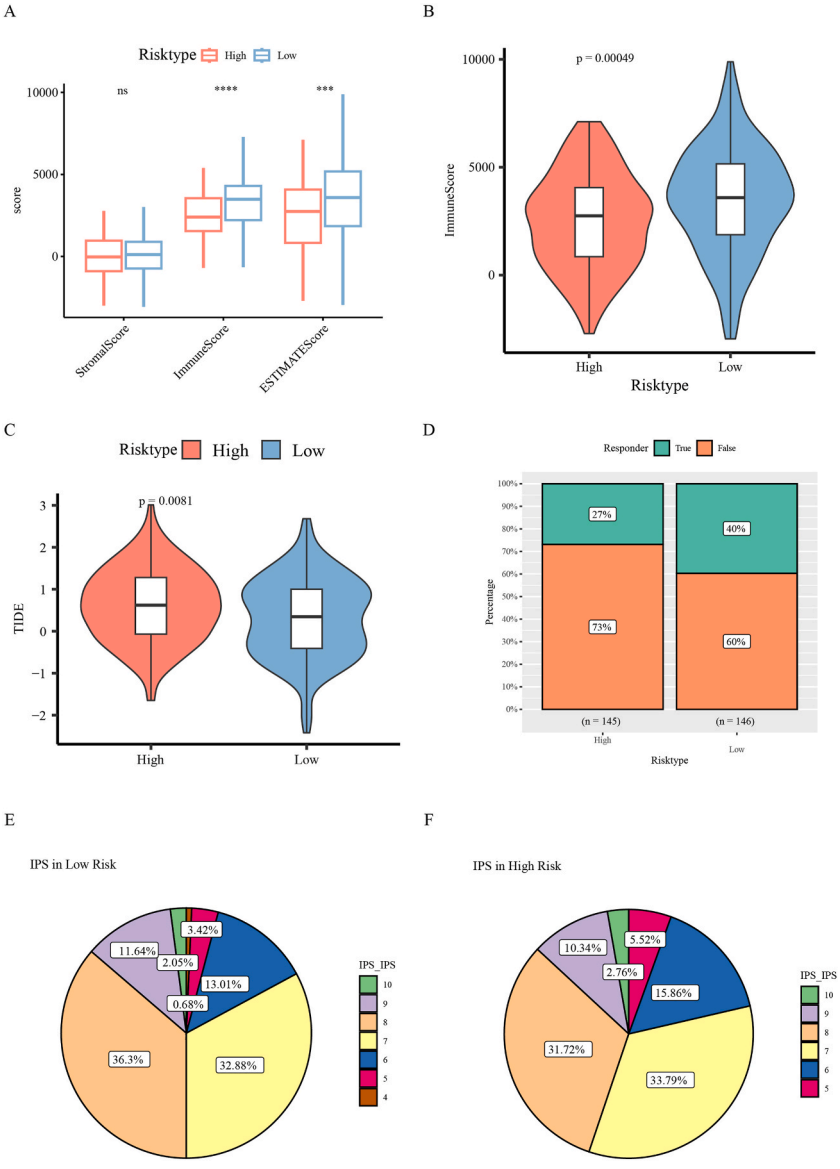

Fig. 5. RiskScore used to predict immunotherapy response in CESC patients.
A: StromalScore, ImmuneScore, ESTIMATEScore of patients in the high and low RiskScore groups. B: Infiltration levels of immune cells in TME of patients in the high and low RiskScore groups. C: TIDE score of patients in the high and low RiskScore groups. D: Statistics of patients' benefit from immunotherapy in the high and low RiskScore groups. E-F: Statistics of IPS scores of patients in the low or high RiskScore group.

3.5. Biological pathways affected by RiskScore

The h.all.v7.5.1.symbols.gmt gene set was finally applied for the gene set enrichment analysis, and abnormal biological pathways in the high and low RiskScore groups were identified. It was delineated that cancer-related pathways were significantly activated in the high RiskScore group, including ECM-receptor interaction, Focal adhesion, MicroRNAs in cancer, Protein digestion and absorption, small cell lung cancer (Fig. 6A). The low RiskScore group was enriched in immune-related pathways, Allograft rejection, Autoimmune thyroid disease, Metabolism of xenobiotics by cytochrome P450, Primary immunodeficiency, and *Staphylococcus aureus* infection (Fig. 6B).

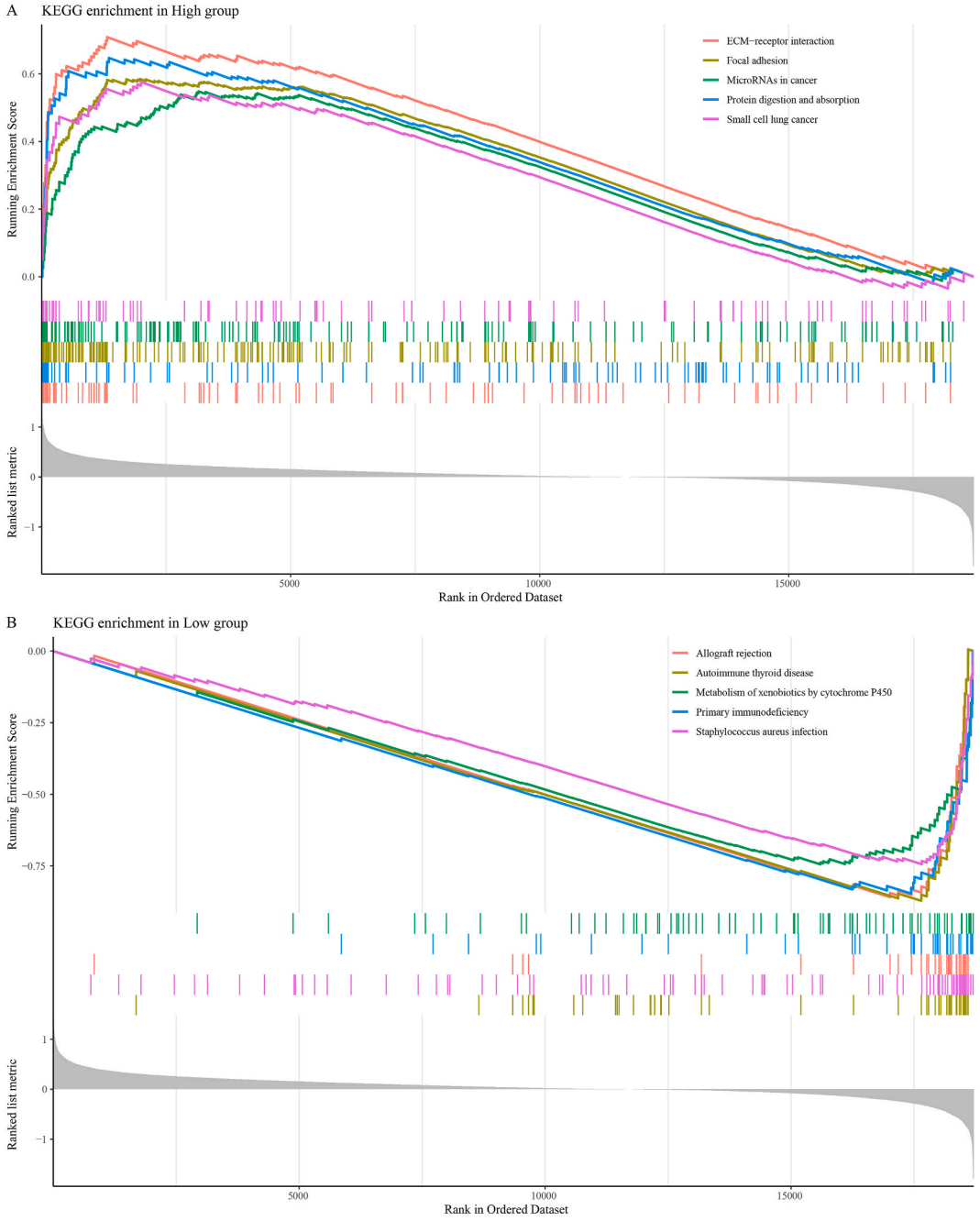

Fig. 6. Biological pathways affected by RiskScore.
A-B: Significantly relevant biological pathways in patients of the high or low RiskScore group.

3.6. Cell validation in cervical cancer cells

In order to preliminarily explore the involvement of the 7 key genes in cervical cancer, their mRNA expressions were tested in both cervical cancer cells Hela and the normal HcerEpic. Notably, the expressions of all 7 key genes were elevated in Hela cells (Fig. 7A). Given the pronounced difference in DLL4 mRNA expression between the tumor group and the control group, coupled with its relevance to angiogenesis and the prognosis of CESC, scratch assay and transwell assay experiments were performed after DLL4 was silenced. The results have suggested that the silencing of DLL4 could significantly weaken the migration and invasion potential of cervical cancer cells Hela, as seen by the reduced wound closure degree and the number of invaded cells at 48 h (Fig. 7B and C).

Furthermore, to further demonstrate whether DLL4 is related to the previously obtained high-risk enrichment pathways (ECM-receptor interaction, Focal adhesion, MicroRNAs in cancer, Protein digestion and absorption, small cell lung cancer), we silenced DLL4 to explore its effect on downstream genes of the MicroRNAs in cancer related pathway. The results showed that the expressions of miR-21 downstream genes PDCD4 and PTEN, as well as miR-34a downstream genes BCL-2 and CDK6, were significantly increased after DLL4 was silenced ($p < 0.05$, Fig. 8). Since miR-21 and miR-34a usually function by negatively regulating their target genes, this result also proves that DLL4 promotes the MicroRNAs in cancer pathway in cervical cancer cells.

4. Discussion

Cervical cancer is showing an increasing trend in morbidity and mortality, and effective prevention and precision guidance are important measures to improve survival. In cancer, vascular survival is particularly important because tumors depend on neovascularization to provide essential oxygen and nutrients to sustain their growth and spread. In this study, three molecular subtypes were identified by vascular survival genes, and finally, a prognostic model of seven related genes was developed. Such a robust model is independent of clinicopathologic features.

Three molecular subtypes were identified in the TCGA-CESC dataset: and these subtypes exhibited different survival advantages and gene expression patterns. Specifically, the C2 subtype showed the best survival advantage, whereas the C1 subtype showed a poorer prognosis. Specifically, we disclosed that cancer-associated pathways (TGF_BETA_SIGNALING, ANGIOGENESIS, G2M_CHECKPOINT, IL6_JAK_STAT3_SIGNALING, KRAS_SIGNALING_UP) were profoundly activated in the C1 subtype. TGF BETA SIGNALING was an important biological pathway in cancer development and cell migration [34]. Angiogenesis, the process of forming new capillaries in cancer cells, is an important source of oxygen and nutrients in tumor cells and an important driver of cancer progression [35]. Inhibition of Angiogenesis has also been shown to be one of the effective means of treating cancer [35]. The G2/M checkpoint is a key regulatory point in the cell cycle that ensures that the cell repairs DNA damage and maintains genomic integrity before entering mitosis. Under normal conditions, the G2/M checkpoint serves as an anti-cancer mechanism that protects cells from DNA damage by maintaining the correct sequence and timing of cell division. However, many cancer cells exhibit resistance to this checkpoint, allowing cells with genetic defects to undergo mitosis and proliferate [36,37]. IL-6 is a cytokine promoting tumor cell proliferation and survival through activation of JAK and STAT3 [38]. IL-6/JAK/STAT3 signaling pathway is also important in pro-inflammatory and modulating immune responses in the TME. It modulates the activity of tumor-associated macrophages and other immune cells and promotes the production of pro-inflammatory and pro-tumorigenic cytokines and chemokines that maintain and exacerbate the inflammatory environment of the tumor [39]. Importantly, STAT3 activation also enhances the expression level of VEGF, thereby enhancing tumor angiogenesis. This provides tumors with essential oxygen and nutrients to support their growth and spread [40]. KRAS can promote uncontrolled proliferation of tumor cells by activating the downstream ERK/MAPK and PI3K/AKT signaling pathways, which promote the expression of cell cycle proteins and the advancement of the cell cycle [41]. These cancer-associated pathways are activated in C1 and may account for the poorer prognosis of the C1 subtype. In addition, immune infiltration analysis of the C1 subtype showed higher ImmuneScore and ESTIMATEScore. ImmuneScore is generally used to quantify the infiltration degree of immune cells in tumor samples. The C1 subtype, with a higher ImmuneScore, likely indicates a higher density of immune cells within the tumor. Meanwhile, ESTIMATEScore is a comprehensive indicator that assesses the relative proportion and activity of stromal cells and immune cells in the TME. The high ESTIMATEScore of the C1 subtype suggests that its TME not only contains more immune cells but may also be accompanied by changes in stromal cells. In conclusion, the C1 subtype possesses a more

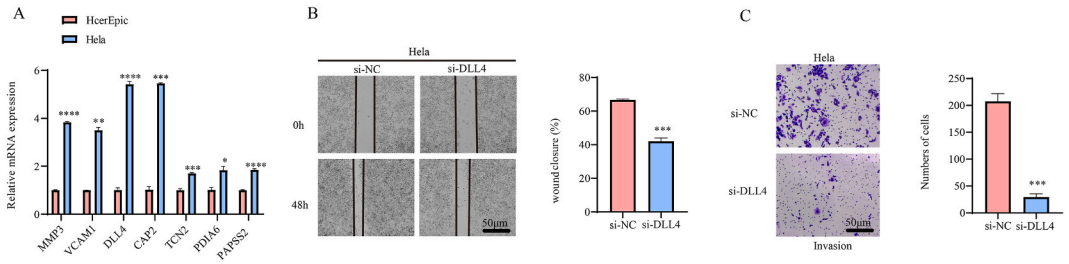

Fig. 7. Cell validation in cervical cancer cells.
A: Relative mRNA levels of key genes affecting prognosis in cervical cancer cells Hela and normal human cervical epithelial cells. B: The migration of cervical cancer cells following the knockdown of DLL4. C: The invasion of cervical cancer cells following the knockdown of DLL4.

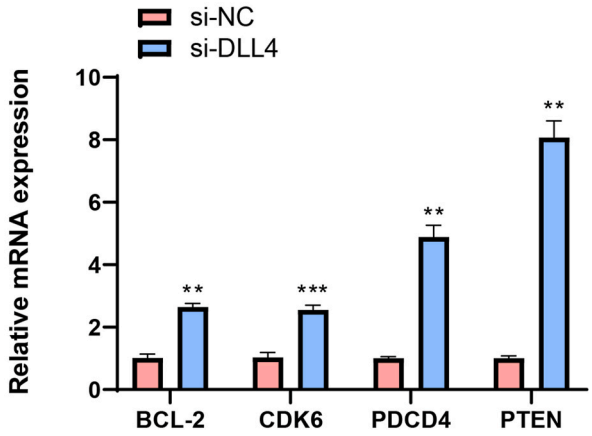

Fig. 8. Performing *in vitro* validation of the MicroRNAs in cancer pathway.

complex immune microenvironment, which may also be one of the reasons for its poorer prognosis.

Risk assessment models for seven prognosis-related genes (TCN2, VCAM1, MMP3, CAP2, DLL4, PDIA6, PAPSS2) showed good predictive performance and consistent trends in the two separate sets and the entire TCGA-CESC cohort. The expression levels of these genes were significantly correlated with the survival of CESC patients, with patients in the high-risk scoring group showing a poorer survival. VCAM1 is a vascular cell adhesion molecule, and it has been found that VCAM1, targeted and inhibited by miR-95-3p, is involved in cervical cancer progression [42]. MMP9 is a molecular signature of lymph node micrometastasis in cervical cancer, with an upregulated level in cervical cancer patients with such micrometastasis [43]. Polarized M2 macrophages induce pre-metastatic microhabitat formation and promote gastric cancer cell metastasis by secreting TGFB1, which generates a TGFB1/JUN/CAP2 positive feedback loop to sustainably activate expression of CAP2, a potential target for cancer metastasis [44]. PDIA6 promotes the development of endometrial cancer through activation of the TGF-β pathway [44]. Han et al. recognized PAPSS2 as a methylation/hydroxymethylation-related gene affecting the prognosis of cervical cancer [45]. DLL4 was identified as both an indicator for the detection of pelvic lymph node metastasis and a prognostic biomarker in patients with early cervical cancer [46]. During angiogenesis, DLL4 binds to Notch receptors, activating the Notch signaling pathway, which in turn regulates the proliferation, migration, and differentiation of vascular endothelial cells [47]. This signaling pathway has been proven to be associated with the prognosis of CESC [48]. Relevant cellular *in-vitro* assays have further uncovered the elevated expressions of these 7 genes in cervical cancer cells Hela, as well as the weakened invasion and migration capabilities of Hela cells after DLL4 silencing. The regulation of these genes reveals key molecular mechanisms in the pathologic process of cervical cancer and provide a theoretical basis for the development of therapeutic strategies against these molecular targets.

The RiskScore was applied to assess the likely response of patients to immunotherapy, where patients in the low RiskScore group exhibited higher ImmuneScore and lower TIDE scores, suggesting that these patients may be more sensitive to immunotherapy. Yang et al. have discovered that in cervical cancer patients with high risk, immune-related genes may reflect the dynamically changing TME [49]. Prior studies have shown that compared to normal tissues, T cells CD4 memory resting, Monocytes, Macrophage M2, and Mast cells resting constitute a smaller proportion in tumor samples, while T cells follicular helper and Macrophages M0 account for a larger proportion, suggesting the influence of tumor cells on immune infiltration [50]. Furthermore, a higher proportion of patients with high IPS scores were observed in the low-risk scoring group. The elevation of IPS is primarily attributed to enhanced antigen-presenting capabilities within the TME, increased infiltration of effector cells (such as activated $CD4^+$ and $CD8^+$ T cells, effector memory T cells, etc.), and reduced infiltration of immunosuppressive cells (like regulatory T cells and myeloid-derived suppressor cells) [30]. Additionally, upregulated expression of major histocompatibility complex (MHC) molecules and related immune regulatory molecules also contributes to the increase in IPS scores [30]. These factors act in concert, making patients with high IPS scores more likely to respond positively to immunotherapies such as immune checkpoint blockade therapies. This finding provides potential biomarkers for individualized treatment of cervical cancer patients, aiding in the optimization of therapeutic strategies.

Additionally, our study has identified significant activation of multiple signaling pathways in the high-risk group patients, which are intimately linked to cancer growth, invasion, and metastasis. These pathways include ECM-receptor interaction, a critical regulator of interactions between the extracellular matrix and cell surface, playing pivotal roles in cell-to-cell communication, proliferation, adhesion, and migration [51]. Furthermore, the enhancement of focal adhesion pathway may facilitate tumor cell adhesion to surrounding tissues, contributing to the development of malignancy characteristics such as cancer stemness, epithelial-mesenchymal transition (EMT), tumor angiogenesis, chemotherapy resistance, and fibrosis in the stroma [52,53]. And the dysregulation of microRNAs signaling is implicated in numerous diseases, including cancer [54]. The *in vitro* validation experiments in this study found that the expressions of miR-21 downstream genes PDCD4 and PTEN, as well as miR-34a downstream genes BCL-2 and CDK6, were all higher in the DLL4-silenced group compared to the control group ($p < 0.05$). PDCD4, a tumor suppressor protein, functions by inhibiting various signaling pathways related to cell growth, proliferation, and survival. A significant downregulation of PDCD4 has been observed in cervical cancer [55]. Furthermore, miR-21 may promote the proliferation of cervical cancer cells by inhibiting the

expression of PTEN [56]. BCL-2, an anti-apoptotic protein, when upregulated, inhibits apoptosis, potentially contributing to enhanced cell proliferation, migration, and invasion [57]. CDK6, a protein kinase belonging to the family of cell cycle regulators, is directly targeted by miR-34a, resulting in its inhibition [58]. These findings all suggest that the MicroRNAs in cancer pathway is suppressed under DLL4 silencing conditions, further validating the role of DLL4 as a biomarker in cervical cancer. In stark contrast, the low-risk group patients exhibit an enrichment of immune-related signaling pathways, such as allograft rejection and autoimmune thyroid disease, which reflect the robust recognition and elimination capability of the body towards 'non-self' components [59,60], a process that is equally crucial in tumor immune surveillance. And cytochrome P450, a membrane-bound heme protein, plays a fundamental role in drug detoxification, cellular metabolism, and homeostasis [61]. Research has demonstrated that the CYP4A/20-HETE axis plays a key role in promoting tumor growth, angiogenesis, migration, and invasion, presenting itself as a potential target for the prevention and treatment of metastasis [62]. This revelation of differing enriched pathways between high- and low-risk groups not only deepens our understanding of cervical cancer but also provides new possibilities for personalized treatment.

However, the present study is not without limitations. Firstly, we did not conduct further experiments to investigate whether silencing DLL4 affects the expression of downstream genes in relevant pathways in the high-risk group, thereby limiting our understanding of its comprehensive biological consequences. Secondly, the relatively small sample size employed in this study introduces a degree of uncertainty and potential bias, limiting the robustness and reproducibility of our findings. Thirdly, the lack of drug sensitivity analysis restricts the application of our results in clinical drug selection. Therefore, in future studies, we will endeavor to increase the sample size to enhance the accuracy of our experiments. Additionally, we will conduct further experimental validations of the relevant biological mechanisms associated with the identified key genes, including downstream pathway analysis and drug sensitivity assays, to provide a more comprehensive insight into the molecular mechanisms underlying cervical cancer development and progression, ultimately facilitating the exploration of more effective therapeutic approaches.

5. Conclusion

In conclusion, by analyzing angiogenesis-related genes in cervical cancer, this study not only identified the subtypes with peculiar biological characteristics and prognoses, but also established an effective prognostic assessment model and explored its potential application in predicting patients' responses to immunotherapy. These results visibly contribute to our understanding of the biological diversity of cervical cancer and provide an important scientific basis for future precision therapy.

Data availability statement

The datasets generated and/or analyzed during the current study are available in the Molecular Signatures Database (MSigDB, https://www.gsea-msigdb.org/gsea/msigdb) database.

Funding

The study was funded by National Science Basic Research Program of Shaanxi Province (No. 2023-JC-YB-655) and Talent Support Funding Program of Shaanxi Provincial People's Hospital (No. 2022BJ-01).

Conflict of interest disclosure

The authors declare that they have no known competing financial interests or personal relationships that could have appeared to influence the work reported in this paper.

Ethics approval statement

Not applicable.

Patient consent statement

Not applicable.

CRediT authorship contribution statement

Zhuo Deng: Writing – review & editing, Writing – original draft, Software, Resources, Methodology, Investigation, Data curation, Conceptualization. **Lu Zhang:** Validation, Supervision, Project administration, Methodology. **Chenyang Sun:** Visualization, Validation, Software, Methodology, Formal analysis. **Yiping Liu:** Validation, Software, Project administration, Methodology, Formal analysis. **Bin Li:** Writing – original draft, Validation, Software, Resources, Methodology, Funding acquisition, Conceptualization.

Declaration of competing interest

The authors declare that they have no known competing financial interests or personal relationships that could have appeared to

influence the work reported in this paper.

Acknowledgments

None.

Abbreviation

CESC	squamous cell carcinoma of the cervix and cervical adenocarcinoma
TCGA	The Cancer Genome Atlas
DEGs	differentially expressed genes
HPV	human papillomavirus
VEGF	vascular endothelial growth factor
MSigDB	Molecular Signatures Database
LASSO COX	Least Absolute Shrinkage and Selection Operator COX
ROC	Receiver Operating Characteristic curve
AUC	Area Under the Curve
TME	tumor microenvironment
TIDE	Tumor Immune Dysfunction and Exclusion
IPS	Immunopheno score
HcerEpic	Human cervical epithelial cell
MHC	major histocompatibility complex
EMT	epithelial-mesenchymal transition

References

[1] P. Shiri Aghbash, N. Hemmat, B. Baradaran, H. Bannazadeh Baghi, siRNA-E6 sensitizes HPV-16-related cervical cancer through Oxaliplatin: an in vitro study on anti-cancer combination therapy, European journal of medical research 28 (1) (2023) 42.
[2] P. Nisha, P. Srushti, D. Bhavarth, M. Kaif, P. Palak, Comprehensive review on analytical and bioanalytical methods for quantification of anti-angiogenic agents used in treatment of cervical cancer, Curr Pharm Anal 19 (10) (2023) 735–744.
[3] R. Wang, W. Pan, L. Jin, W. Huang, Y. Li, D. Wu, et al., Human papillomavirus vaccine against cervical cancer: opportunity and challenge, Cancer Lett. 471 (2020) 88–102.
[4] K.S. Okunade, Human papillomavirus and cervical cancer, J Obstet Gynaecol 40 (5) (2020) 602–608.
[5] S. de Sanjose, W.G.V. Quint, L. Alemany, D.T. Geraets, J.E. Klaustermeier, B. Lloveras, et al., Human papillomavirus genotype attribution in invasive cervical cancer: a retrospective cross-sectional worldwide study, Lancet Oncol. 11 (11) (2010) 1048–1056.
[6] N.R. Abu-Rustum, C.M. Yashar, R. Arend, E. Barber, K. Bradley, R. Brooks, et al., NCCN guidelines(R) insights: cervical cancer, version 1.2024, J Natl Compr Canc Netw 21 (12) (2023) 1224–1233.
[7] A. Halim, W.A. Mustafa, W.K.W. Ahmad, H.A. Rahim, H. Sakeran, Nucleus detection on pap smear images for cervical cancer diagnosis: a review analysis, Oncologie 23 (1) (2021) 73–88.
[8] J.S. Mayadev, G. Ke, U. Mahantshetty, M.D. Pereira, R. Tarnawski, T. Toita, Global challenges of radiotherapy for the treatment of locally advanced cervical cancer, Int. J. Gynecol. Cancer 32 (3) (2022) 436–445.
[9] S. Shen, S. Zhang, P. Liu, J. Wang, H. Du, Potential role of microRNAs in the treatment and diagnosis of cervical cancer, Cancer Genet. 248–249 (2020) 25–30.
[10] C. Chargari, K. Peignaux, A. Escande, S. Renard, C. Lafond, A. Petit, et al., Radiotherapy of cervical cancer, Cancer Radiother. : journal de la Societe francaise de radiotherapie oncologique. 26 (1–2) (2022) 298–308.
[11] M.K. Sundaram, A.G. Almutary, S. Haque, F. Sm, A. Hussain, Awareness of human papilloma virus and its association with cervical cancer among female university students: a study from United Arab Emirates, Oncologie 23 (2) (2021).
[12] M. Schubert, D.O. Bauerschlag, M.Z. Muallem, N. Maass, I. Alkatout, Challenges in the diagnosis and individualized treatment of cervical cancer, Medicina (Kaunas) 59 (5) (2023).
[13] L. Ferrall, K.Y. Lin, R.B.S. Roden, C.F. Hung, T.C. Wu, Cervical cancer immunotherapy: facts and hopes, Clin. Cancer Res. 27 (18) (2021) 4953–4973.
[14] Y. Wu, B. Qu, H. Shen, H. Deng, F. Tang, Serum level of tumor-specific growth factor in patients with cervical cancer and its potential prognostic role, Oncologie 24 (3) (2022).
[15] F.M. Correa, A. Migowski, L.M. de Almeida, M.A. Soares, Cervical cancer screening, treatment and prophylaxis in Brazil: current and future perspectives for cervical cancer elimination, Front. Med. 9 (2022) 945621.
[16] A.S. Oguntade, F. Al-Amodi, A. Alrumayh, M. Alobaida, M. Bwalya, Anti-angiogenesis in cancer therapeutics: the magic bullet, J Egypt Natl Canc Inst 33 (1) (2021) 15.
[17] R.I. Teleanu, C. Chircov, A.M. Grumezescu, D.M. Teleanu, Tumor angiogenesis and anti-angiogenic strategies for cancer treatment, J. Clin. Med. 9 (1) (2019).
[18] Z.L. Liu, H.H. Chen, L.L. Zheng, L.P. Sun, L. Shi, Angiogenic signaling pathways and anti-angiogenic therapy for cancer, Signal Transduct Target Ther 8 (1) (2023) 198.
[19] F. Lopes-Coelho, F. Martins, S.A. Pereira, J. Serpa, Anti-angiogenic therapy: current challenges and future perspectives, Int. J. Mol. Sci. 22 (7) (2021).
[20] Y. Cao, R. Langer, N. Ferrara, Targeting angiogenesis in oncology, ophthalmology and beyond, Nat. Rev. Drug Discov. 22 (6) (2023) 476–495.
[21] X.W. Wei, Z.R. Zhang, Y.Q. Wei, Anti-angiogenic drugs currently in Phase II clinical trials for gynecological cancer treatment, Expert Opin Inv Drug 22 (9) (2013) 1181–1192.
[22] N. Bizzarri, V. Ghirardi, F. Alessandri, P.L. Venturini, M. Valenzano Menada, S. Rundle, et al., Bevacizumab for the treatment of cervical cancer, Expert Opin Biol Th 16 (3) (2016) 407–419.
[23] M.D. Wilkerson, D.N. Hayes, ConsensusClusterPlus: a class discovery tool with confidence assessments and item tracking, Bioinformatics 26 (12) (2010) 1572–1573.
[24] M.E. Ritchie, B. Phipson, D. Wu, Y. Hu, C.W. Law, W. Shi, et al., Limma powers differential expression analyses for RNA-sequencing and microarray studies, Nucleic Acids Res. 43 (7) (2015) e47.

[25] N. Simon, J. Friedman, T. Hastie, R. Tibshirani, Regularization paths for cox's proportional hazards model via coordinate descent, J Stat Softw 39 (5) (2011) 1–13.
[26] P. Blanche, J.F. Dartigues, H. Jacqmin-Gadda, Estimating and comparing time-dependent areas under receiver operating characteristic curves for censored event times with competing risks, Stat. Med. 32 (30) (2013) 5381–5397.
[27] Y. He, Z. Jiang, C. Chen, X. Wang, Classification of triple-negative breast cancers based on Immunogenomic profiling, Journal of experimental & clinical cancer research : CR 37 (1) (2018) 327.
[28] S. Hanzelmann, R. Castelo, J. Guinney, GSVA: gene set variation analysis for microarray and RNA-seq data, BMC Bioinf. 14 (2013) 7.
[29] K. Yoshihara, M. Shahmoradgoli, E. Martinez, R. Vegesna, H. Kim, W. Torres-Garcia, et al., Inferring tumour purity and stromal and immune cell admixture from expression data, Nat. Commun. 4 (2013) 2612.
[30] P. Charoentong, F. Finotello, M. Angelova, C. Mayer, M. Efremova, D. Rieder, et al., Pan-cancer immunogenomic analyses reveal genotype-immunophenotype relationships and predictors of response to checkpoint blockade, Cell Rep. 18 (1) (2017) 248–262.
[31] D. Zeng, Z. Ye, R. Shen, G. Yu, J. Wu, Y. Xiong, et al., IOBR: multi-omics immuno-oncology biological research to decode tumor microenvironment and signatures, Front. Immunol. 12 (2021) 687975.
[32] K.J. Livak, T.D. Schmittgen, Analysis of relative gene expression data using real-time quantitative PCR and the 2(-Delta Delta C(T)) Method, Methods 25 (4) (2001) 402–408.
[33] S. Amuthalakshmi, S. Sindhuja, C.N. Nalini, A review on PCR and POC-PCR - a boon in the diagnosis of COVID-19, Curr Pharm Anal 18 (8) (2022) 745–764.
[34] M. Zhao, L. Mishra, C.X. Deng, The role of TGF-beta/SMAD4 signaling in cancer, Int. J. Biol. Sci. 14 (2) (2018) 111–123.
[35] M. Farhan, M. Silva, X. Xingan, Y. Huang, W. Zheng, Role of FOXO transcription factors in cancer metabolism and angiogenesis, Cells 9 (7) (2020).
[36] M. Oshi, H. Takahashi, Y. Tokumaru, L. Yan, O.M. Rashid, R. Matsuyama, et al., G2M cell cycle pathway score as a prognostic biomarker of metastasis in estrogen receptor (ER)-Positive breast cancer, Int. J. Mol. Sci. 21 (8) (2020).
[37] K. Engeland, Cell cycle arrest through indirect transcriptional repression by p53: I have a DREAM, Cell Death Differ. 25 (1) (2018) 114–132.
[38] G.G. Eskiler, E. Bezdegumeli, Z. Ozman, A.D. Ozkan, C. Bilir, B.N. Kucukakca, et al., IL-6 mediated JAK/STAT3 signaling pathway in cancer patients with cachexia, Bratisl. Lek. Listy 66 (11) (2019) 819–826.
[39] S.G. Manore, D.L. Doheny, G.L. Wong, H.W. Lo, IL-6/JAK/STAT3 signaling in breast cancer metastasis: biology and treatment, Frontiers in oncology 12 (2022) 866014.
[40] S. Qiao, Y. Hou, Q. Rong, B. Han, P. Liu, Tregs are involved in VEGFA/VASH1-related angiogenesis pathway in ovarian cancer, Transl Oncol 32 (2023) 101665.
[41] M.G. Ferrara, A. Stefani, S. Pilotto, C. Carbone, E. Vita, M. Di Salvatore, et al., The renaissance of KRAS targeting in advanced non-small-cell lung cancer: new opportunities following old failures, Frontiers in oncology 11 (2021) 792385.
[42] S. Feng, Y. Lu, L. Sun, S. Hao, Z. Liu, F. Yang, et al., MiR-95-3p acts as a prognostic marker and promotes cervical cancer progression by targeting VCAM1, Ann. Transl. Med. 10 (21) (2022) 1171.
[43] T. Hagemann, T. Bozanovic, S. Hooper, A. Ljubic, V.I. Slettenaar, J.L. Wilson, et al., Molecular profiling of cervical cancer progression, Br. J. Cancer 96 (2) (2007) 321–328.
[44] G. Zhang, Z. Gao, X. Guo, R. Ma, X. Wang, P. Zhou, et al., CAP2 promotes gastric cancer metastasis by mediating the interaction between tumor cells and tumor-associated macrophages, J. Clin. Invest. 133 (21) (2023).
[45] Y. Han, L. Ji, Y. Guan, M. Ma, P. Li, Y. Xue, et al., An epigenomic landscape of cervical intraepithelial neoplasia and cervical cancer using single-base resolution methylome and hydroxymethylome, Clin. Transl. Med. 11 (7) (2021) e498.
[46] S. Yang, Y. Liu, B. Xia, J. Deng, T. Liu, Q. Li, et al., DLL4 as a predictor of pelvic lymph node metastasis and a novel prognostic biomarker in patients with early-stage cervical cancer, Tumour Biol 37 (4) (2016) 5063–5074.
[47] I. Lobov, N. Mikhailova, The role of Dll4/Notch signaling in normal and pathological ocular angiogenesis: dll4 controls blood vessel sprouting and vessel remodeling in normal and pathological conditions, J Ophthalmol. 2018 (1) (2018) 3565292.
[48] M. Khelil, H. Griffin, M.C.G. Bleeker, R.D.M. Steenbergen, K. Zheng, T. Saunders-Wood, et al., Delta-like ligand–notch1 signaling is selectively modulated by HPV16 E6 to promote squamous cell proliferation and correlates with cervical cancer prognosis, Cancer Res. 81 (7) (2021) 1909–1921.
[49] S. Yang, Y. Wu, Y. Deng, L. Zhou, P. Yang, Y. Zheng, et al., Identification of a prognostic immune signature for cervical cancer to predict survival and response to immune checkpoint inhibitors, OncoImmunology 8 (12) (2019) e1659094.
[50] L. Yang, Y. Yang, M. Meng, W. Wang, S. He, Y. Zhao, et al., Identification of prognosis-related genes in the cervical cancer immune microenvironment, Gene 766 (2021) 145119.
[51] S. Nersisyan, V. Novosad, N. Engibaryan, Y. Ushkaryov, S. Nikulin, A. Tonevitsky, ECM–Receptor regulatory network and its prognostic role in colorectal cancer, Front. Genet. 12 (2021).
[52] J.M. Murphy, Y.A.R. Rodriguez, K. Jeong, E.-Y.E. Ahn, S.-T.S. Lim, Targeting focal adhesion kinase in cancer cells and the tumor microenvironment, Exp. Mol. Med. 52 (6) (2020) 877–886.
[53] B.Y. Lee, P. Timpson, L.G. Horvath, R.J. Daly, FAK signaling in human cancer as a target for therapeutics, Pharmacol. Ther. 146 (2015) 132–149.
[54] S. Cai, T. Pataillot-Meakin, A. Shibakawa, R. Ren, C.L. Bevan, S. Ladame, et al., Single-molecule amplification-free multiplexed detection of circulating microRNA cancer biomarkers from serum, Nat. Commun. 12 (1) (2021) 3515.
[55] S. Bumrungthai, T. Ekalaksananan, M.F. Evans, P. Chopjitt, T. Tangsiriwatthana, N. Patarapadungkit, et al., Up-regulation of miR-21 is associated with cervicitis and human papillomavirus infection in cervical tissues, PLoS One 10 (5) (2015) e0127109.
[56] J. Xu, W. Zhang, Q. Lv, D. Zhu, Overexpression of miR-21 promotes the proliferation and migration of cervical cancer cells via the inhibition of PTEN, Oncol. Rep. 33 (6) (2015) 3108–3116.
[57] X. Wang, Y. Xie, J. Wang, Overexpression of MicroRNA-34a-5p inhibits proliferation and promotes apoptosis of human cervical cancer cells by downregulation of bcl-2, Oncol. Res. 26 (6) (2018) 977–985.
[58] F. Sun, H. Fu, Q. Liu, Y. Tie, J. Zhu, R. Xing, et al., Downregulation of CCND1 and CDK6 by miR-34a induces cell cycle arrest, FEBS (Fed. Eur. Biochem. Soc.) Lett. 582 (10) (2008) 1564–1568.
[59] M.Y. Kim, D.C. Brennan, Therapies for chronic allograft rejection, Front. Pharmacol. 12 (2021).
[60] P.S. Heeger, M.C. Haro, S. Jordan, Translating B cell immunology to the treatment of antibody-mediated allograft rejection, Nat. Rev. Nephrol. 20 (4) (2024) 218–232.
[61] M. Zhao, J. Ma, M. Li, Y. Zhang, B. Jiang, X. Zhao, et al., Cytochrome P450 enzymes and drug metabolism in humans, Int. J. Mol. Sci. 22 (23) (2021) 12808.
[62] B. Luo, D. Yan, H. Yan, J. Yuan, Cytochrome P450: implications for human breast cancer, Oncol. Lett. 22 (1) (2021) 548 (Review).